PCCP

ROYAL SOCIETY OF CHEMISTRY

PAPER

Cite this: *Phys. Chem. Chem. Phys.*, 2023, **25**, 17460

Synthesis of interstellar propen-2-ol ($CH_3C(OH)CH_2$) – the simplest enol tautomer of a ketone†

Jia Wang, [ab] Anatoliy A. Nikolayev, [c] Chaojiang Zhang,[ab] Joshua H. Marks, [ab] Valeriy N. Azyazov,[d] André K. Eckhardt, *[e] Alexander M. Mebel *[f] and Ralf I. Kaiser *[ab]

Enols – tautomers of ketones or aldehydes – are anticipated to be ubiquitous in the interstellar medium and play a key role in the formation of complex organic molecules in deep space, but their fundamental formation mechanisms have remained largely elusive as of now. Here we present a combined experimental and computational study demonstrating the first preparation of propen-2-ol ($CH_3C(OH)CH_2$) and its isomer methyl vinyl ether (CH_3OCHCH_2) in low-temperature acetone (CH_3COCH_3) ices upon exposure to energetic electrons. Propen-2-ol is the simplest enol tautomer of a ketone. Exploiting tunable vacuum ultraviolet photoionization in conjunction with reflectron time-of-flight mass spectrometry, propen-2-ol and methyl vinyl ether were monitored in the gas phase upon sublimation during the temperature-programmed desorption process suggesting that both isomers are promising candidates for future astronomical searches such as *via* the James Webb Space Telescope. Electronic structure calculations reveal that the barrier of keto–enol tautomerization can be reduced by more than a factor of two (162 kJ mol^{-1}) through the involvement of solvating water molecules under realistic conditions on interstellar grains. The implicit solvent effects, *i.e.*, the influences of the solvent dipole field on the barrier height are found to be minimal and do not exceed 10 kJ mol^{-1}. Our findings signify a crucial step toward a better understanding of the enolization of ketones in the interstellar medium thus constraining the molecular structures and complexity of molecules that form in extraterrestrial ices - ketones - through non-equilibrium chemistry.

Received 21st May 2023,
Accepted 16th June 2023

DOI: 10.1039/d3cp02307a

rsc.li/pccp

Introduction

Since the recognition of enols as tautomers of ketones or aldehydes by Erlenmeyer more than a century ago,[1] enols have received considerable attention from the synthetic organic chemistry,[2] combustion chemistry,[3] atmospheric chemistry,[4] physical chemistry,[5] theoretical chemistry,[6] and astrochemistry[7–10] communities. This interest is mainly due to their role as reactive intermediates in molecular mass growth processes which can produce sugars (interstellar medium),[9–11] volatile organic compounds (atmospheric chemistry),[12] and ethers (combustion processes).[13] Whereas in the liquid phase, thermodynamically less stable enols such as vinyl alcohol (CH_2CHOH) exist as transients in concentrations as low as 6×10^{-8} in equilibrium with their aldehyde tautomer acetaldehyde (CH_3CHO),[14] in the interstellar medium (ISM), vinyl alcohol (CH_2CHOH) to acetaldehyde (CH_3CHO) ratios close to unity have been observed toward the star forming region of Sagittarius B2 (Sgr B2).[15] This is the consequence of a galactic cosmic ray (GCR) triggered non-equilibrium processing of ice-coated nanoparticles in the molecular cloud stage.[9,10] Laboratory simulation experiments revealed a facile synthesis of the acetaldehyde (CH_3CHO) – vinyl alcohol (CH_2CHOH, +41 kJ mol^{-1}),[7] ketene (H_2CCO) – ethynol (HCCOH, +140 kJ mol^{-1}),[16] pyruvic acid ($CH_3COCOOH$) – 2-hydroxyacrylic acid ($CH_2C(OH)COOH$, +28 kJ mol^{-1}),[8] acetic acid (CH_3COOH) – 1,1-ethenediol ($H_2CC(OH)_2$, +114 kJ mol^{-1}),[10] and glycolaldehyde ($HCOCH_2OH$)–1,2-ethenediol (H(HO)CC(OH)H, +39 kJ mol^{-1})[9] pairs with relative energies of the enols provided in parentheses

[a] *Department of Chemistry, University of Hawaii at Manoa, Honolulu, HI 96822, USA. E-mail: ralfk@hawaii.edu*
[b] *W. M. Keck Research Laboratory in Astrochemistry, University of Hawaii at Manoa, Honolulu, HI 96822, USA*
[c] *Samara National Research University, Samara 443086, Russia*
[d] *Lebedev Physical Institute, Samara 443011, Russia*
[e] *Lehrstuhl für Organische Chemie II, Ruhr-Universität Bochum, Bochum 44801, Germany. E-mail: Andre.Eckhardt@ruhr-uni-bochum.de*
[f] *Department of Chemistry and Biochemistry, Florida International University, Miami, Florida 33199, USA. E-mail: mebela@fiu.edu*

† Electronic supplementary information (ESI) available: Ion signal of higher masses and assignment, Fig. S1–S6, Tables S1–S9. See DOI: https://doi.org/10.1039/d3cp02307a

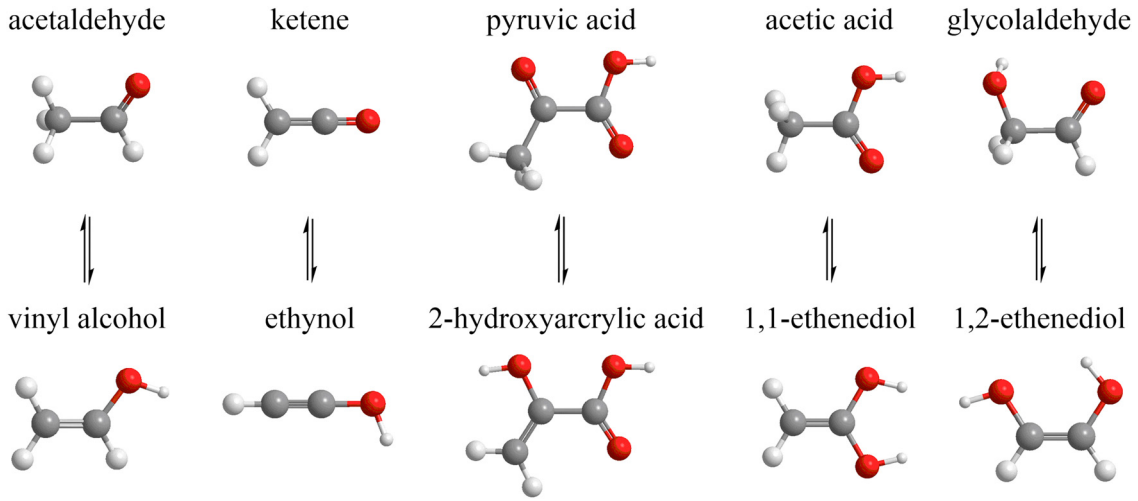

Scheme 1 Tautomer pairs observed in interstellar analog ices subjected to ionizing radiation.

(Scheme 1), suggesting that enols may be ubiquitous in deep space and readily available for an abiotic synthesis of complex organic molecules in these extreme environments.[8–10,17] However, as of today, only vinyl alcohol (CH_2CHOH) and 1,2-ethenediol ($H_2CC(OH)_2$) have been identified in deep space.[15,18] The enol of the simplest ketone acetone (**1**, CH_3COCH_3)–propen-2-ol (**2**, $CH_3C(OH)CH_2$) – has remained elusive in the interstellar medium, but its identification could provide fundamental constraints of the chemical and physical conditions of cold molecular clouds and star-forming regions as their descendants.[2,19–22]

On Earth, propen-2-ol (**2**) has been identified as a transient during the photolysis of 2-pentanone ($CH_3COC_3H_7$)[2,22] and 1-methylcyclobutanol ($C_5H_{10}O$)[20] as intermediates of the photon-initiated reaction of acetone in 2-propanol ($(CH_3)_2CHOH$)[19] and of electron processed acetone–argon gas mixtures.[21] However, preparation of propen-2-ol (**2**) in astrophysically relevant ices has not yet been accomplished to date despite investigations of acetone ices exposed to atomic hydrogen,[23] energetic ions (40 MeV $^{58}Ni^{11+}$),[24] protons (1 MeV),[25] or X-ray.[26] Propen-2-ol (**2**) together with the methyl vinyl ether isomer (**4**, CH_3OCHCH_2) have been the target of a computational study through the isomerization of acetone (**1**) (Fig. 1),[6,27] but experimental evidence on the interconversion of acetone (**1**) to propen-2-ol (**2**) under astrophysical conditions is still lacking. Therefore, a high-level experimental study is warranted to trigger the tautomerization of acetone (**1**) and to identify propen-2-ol (**2**) in low temperature ices.

Here, we present laboratory experiments on the preparation of the astronomically elusive propen-2-ol (**2**) and methyl vinyl ether (**4**) in low-temperature acetone (**1**) ices *via* processing by ionizing radiation in the form of energetic electrons at 5 K. These electrons simulate secondary electrons generated in the track of GCRs and replicate energetic processing of interstellar analog ices over interstellar timescales of a few 10^5 years.[28] Photoionization reflectron time-of-flight mass spectrometry (PI-ReToF-MS) in conjunction with isotopically labeled ices was exploited to identify propen-2-ol (**2**) and methyl vinyl ether (**4**) upon sublimation of the exposed ices in the gas phase *via* fragment-free *isomer-specifically* photoionization during the temperature-programmed desorption (TPD) phase. Acetone (**1**) was the first ten-atom molecule detected in the interstellar medium by the IRAM 30 m and NRAO 12 m telescopes[29] with fractional abundances of up to 3×10^{-9} with respect to molecular hydrogen (H_2) in Sgr B2.[30] A recent survey by the James Webb Space Telescope (JWST) tentatively identified acetone (**1**) in ices toward the stars NIR38 and J110621.[31] The nucleophilic character and, hence, boosted reactivity of propen-2-ol (**2**) compared to acetone (**1**)[10] might have far reaching consequences, such as propen-2-ol (**2**) serving as a reactive intermediate for, *e.g.*, aldol reactions eventually forming complex organics[9] including sugar related molecules in our universe.

Experimental and computational

The experiments were carried out in a hydrocarbon-free stainless steel ultrahigh vacuum chamber with pressures maintained at a few 10^{-11} torr.[32] A 12.6 × 15.1 mm polished silver substrate was mounted on an oxygen-free copper cold head and cooled to 5.0 ± 0.2 K using a closed-cycle helium refrigerator (Sumitomo Heavy Industries, RDK-415E). Acetone (CH_3COCH_3, Fisher Chemical, >99.5%) and acetone-d_6 (CD_3COCD_3, CDN Isotopes, 99.9 atom %D) were introduced into the main chamber at a pressure of 3×10^{-8} torr through a glass capillary array (10 mm diameter) and deposited onto the silver substrate. During the deposition, the ice growth was monitored *in situ* with a helium–neon laser (CVI Melles Griot; 25-LHP-230, 632.8 nm) *via* laser interferometry.[33] With the refractive indices of 1.335 ± 0.002 for amorphous acetone at 20 K,[34] the thickness of ice was determined to be 710 ± 30 nm (Table S1, ESI†). FTIR spectra (Thermo Electron, Nicolet 6700, 4 cm^{-1} resolution) of ices were measured in the range of 6000–500 cm^{-1} after deposition. In the ice mixture experiment, the ratio of the CH_3COCH_3–CD_3COCD_3 ice was determined to be (1.1 ± 0.2):1

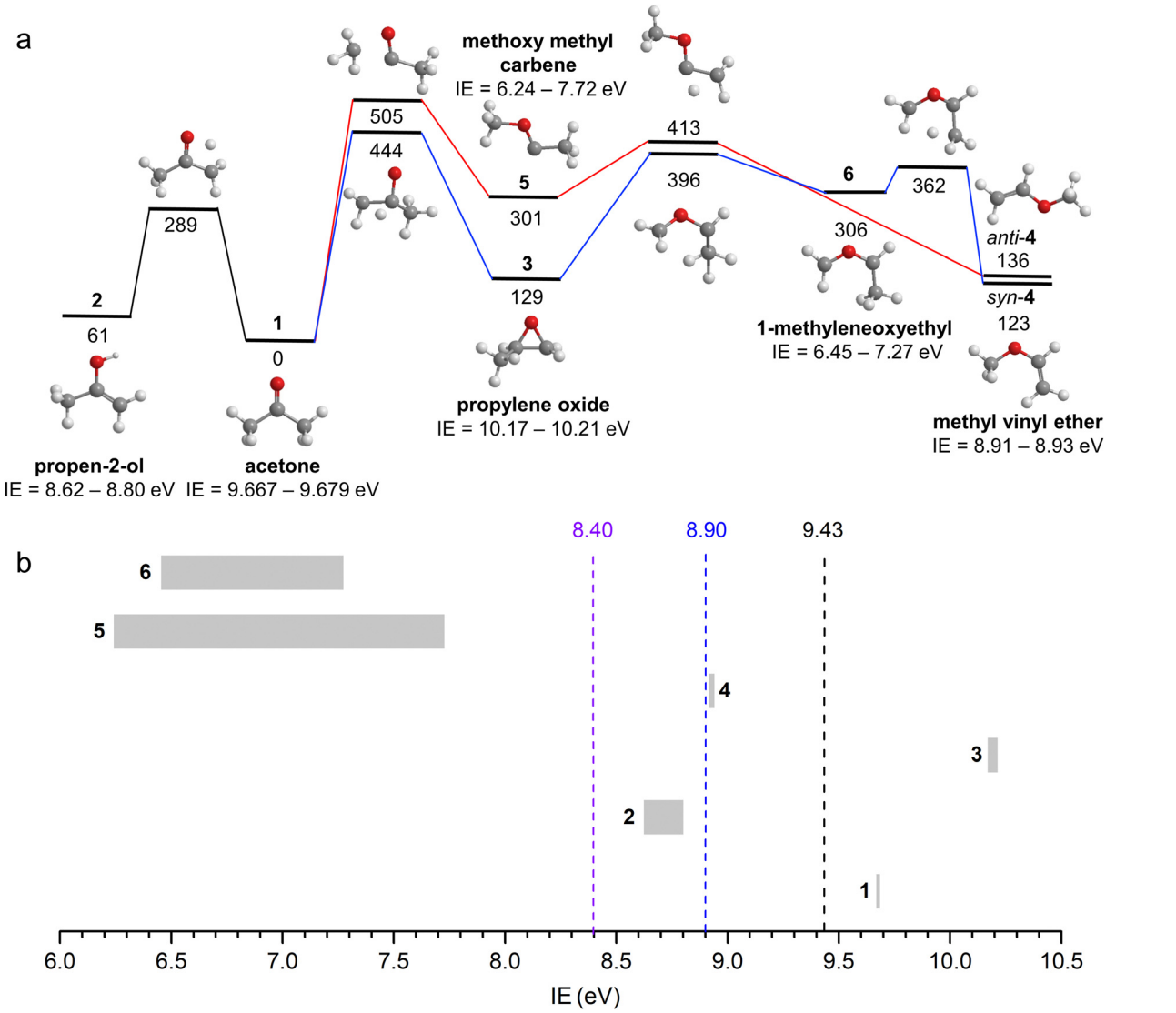

Fig. 1 (a) Isomerization of acetone (**1**) leading to the formation of propen-2-ol (**2**) and methyl vinyl ether (**4**). Energies (kJ mol^{-1}) computed by Elango *et al.* at the MP2/cc-pVDZ level of theory are relative to acetone (**1**).[6] (b) Ranges of adiabatic ionization energies (IE) of selected C_3H_6O isomers after error analysis (Table S3, ESI†). Three VUV photon energies (dash lines) were used to discriminate the sublimating molecules.

by utilizing the absorption bands of their pure ices. After deposition, ices were irradiated with 5 keV electrons (SPECS, EQ PU-22) with a current of 20 nA for 5 minutes or 15 nA for 2 minutes, resulting in a dose of up to 0.40 ± 0.06 eV molecule^{-1} (Table S1, ESI†). These doses are equivalent to 5 × 10^5 years of exposure to GCRs in the interior of a molecular cloud for an interstellar ice grain.[28] Using the densities of 0.783 ± 0.002 g cm^{-3} for amorphous acetone at 20 K,[34] an average penetration depth of 330 ± 20 nm was determined for ices irradiated at 20 nA for 5 minutes according to Monte Carlo simulations using CASINO 2.42.[35] The penetration depth is notably less than the ice thickness (710 ± 30 nm), preventing energetic electron-initiated interactions between the ice and the silver substrate. FTIR spectra were collected before, during, and after irradiation to track changes in the chemical composition.

After irradiation, the ice was heated from 5 to 320 K at a rate of 0.5 K min^{-1} to sublime species. During temperature-programmed desorption (TPD) phase, pulsed vacuum ultraviolet (VUV) source was used to photoionize the subliming species and producing ions, which were then detected by a reflectron time-of-flight mass spectrometer (Jordan TOF Products, Inc.) equipped with two microchannel plates (MCPs). VUV lights at single photon energies of 9.43 eV, 8.90 eV, and 8.40 eV were generated through resonant four-wave mixing ($\omega_{VUV} = 2\omega_1 - \omega_2$) processes of two synchronized pulsed laser beams, which were produced by two dye lasers (Sirah, Cobra-Stretch) pumped by two neodymium-doped yttrium aluminum garnet (Nd:YAG) lasers (Spectra-Physics, Quanta Ray Pro 250–30 and 270–30, 30 Hz). Detailed parameters are listed in Table S2 (ESI†). The generated VUV photons were spatially separated from other photons using a biconvex lithium fluoride lens (Korth Kristalle, $R_1 = R_2 =$ 131 mm) in an off-axis geometry and passed 2 mm above the surface of the ice to photoionize gas-phase molecules. Signals

from the MCP were amplified by a fast preamplifier (Ortec 9305), discriminated by a constant fraction discriminator (Advanced Research Instruments Corp., F100-TD), and recorded by a multichannel scaler (FAST ComTec, MCS6A). Each mass spectrum during the TPD phase was recorded with the accumulation of 2 minutes (3600 sweeps) in bins of 3.2 ns widths. The sublimed molecules were also detected by an electron impact ionization quadrupole mass spectrometer (QMS; Extrel, Model 5221), with 70 eV electron energy. A blank experiment (without electron irradiation) was performed at 9.43 eV to verify that the detected signals were produced by an external energy source. Ion counts were corrected for variations in VUV intensity that was measured during the TPD phase.

All computations were carried out with Gaussian 16, Revision C.01.[36] For geometry optimizations and frequency computations, the B3LYP density functional[37–39] in combination with the triple zeta dunning correlation-consistent basis set cc-pVTZ.[40] Based on these geometries, the corresponding frozen-core coupled cluster[41–44] CCSD(T)/cc-pVTZ and CCSD(T)/cc-pVQZ single point energies were computed and extrapolated to complete basis set limit[45] CCSD(T)/CBS with B3LYP/cc-pVTZ zero-point vibrational energy (ZPVE) corrections. The adiabatic ionization energies were computed from the difference between the ZPVE corrected energies of neutral and ionic states that correspond to similar conformations. As the difference in zero-point vibrational energy between the ground and cationic states changes only marginally with isotopic substitution, we assume the adiabatic ionization energy does not change between the isotopologues of acetone. The error analyses of computed ionization energies of C_3H_6O isomers are listed in Table S3 (ESI†). Due to both temperature-dependent internal energy and the static electric field-induced Stark shift caused by the acceleration field of mass spectrometer, the ionization energies of the molecules decrease by 0.03 eV.[32] Geometries of the reactants, transition states, and products of the acetone–propen-2-ol isomerization reaction without and with several explicit water molecules participating in the H-transfer process were initially optimized at the density functional ωB97X-D/6-311G(d,p) level of theory,[46] with vibrational frequencies and zero-point vibrational energy corrections computed using the same method. For smaller systems including up to two extra H_2O molecules, single-point energies were further refined using the explicitly-correlated coupled cluster CCSD(T)-F12/cc-pVTZ-F12 method.[47,48] The differences in relative energies obtained at the CCSD(T)-F12/cc-pVTZ-F12//ωB97X-D/6-311G(d,p) and ωB97X-D/6-311G(d,p) levels of theory did not exceed 10 kJ mol^{-1} for the reaction products (solvated propen-2-ol) and transitions states, which validates the use of the ωB97X-D/6-311G(d,p) method for the larger systems. Furthermore, the solvation effects for the systems including water molecules were included through self-consistent reaction field (SCRF) – polarizable continuum model (PCM) calculations with water used as implicit solvent.[49] For the $CH_3COCH_3/n(H_2O)$ (n = 1–5) systems geometries were reoptimized and ZPE corrections were computed at the SCRF-PCM/ωB97X-D/6-311G(d,p) level of theory to get the final energies. The SCRF-PCM and ωB97X-D calculations were carried out employing Gaussian 16, whereas the CCSD(T)-F12 calculations were performed utilizing the MOLPRO 2010 package.[50] Computed Cartesian coordinates and vibration frequencies are listed in Tables S8 and S9 (ESI†).

Results and discussion

FTIR spectra

Fourier transform infrared (FTIR) spectra of pure ices of acetone (CH_3COCH_3) and acetone-d_6 (CD_3COCD_3) were collected before, during, and after the exposure to ionizing radiation. Prior to irradiation the spectra are dominated by the C=O stretching mode (ν_3) at 1708 cm^{-1} and 1697 cm^{-1} for acetone and acetone-d_6, respectively (Fig. 2 and Tables S4, S5, ESI†).[34,51] After irradiation, a new feature emerged at 2128 cm^{-1} (Fig. 2a, insert) that can be linked to the CO stretch of carbon monoxide and/or ketene (ν_2, H_2CCO).[26,52] In the acetone-d_6 ice, a new absorption at 2096 cm^{-1} appeared after the electron exposure (Fig. 2b, insert), which may be linked to the CD_3 symmetric stretching mode of propen-2-ol-d_6 (**2**, $CD_3C(OD)CD_2$).[21] However, in the acetone system, the symmetric stretching mode of the methyl group (CH_3) at 2836 cm^{-1} for propen-2-ol (**2**) is masked by the overtone ($2\nu_{21}$, 2854 cm^{-1}) of acetone (**1**).[21] Consequently, the FTIR data only tentatively identify functional groups which might be associated

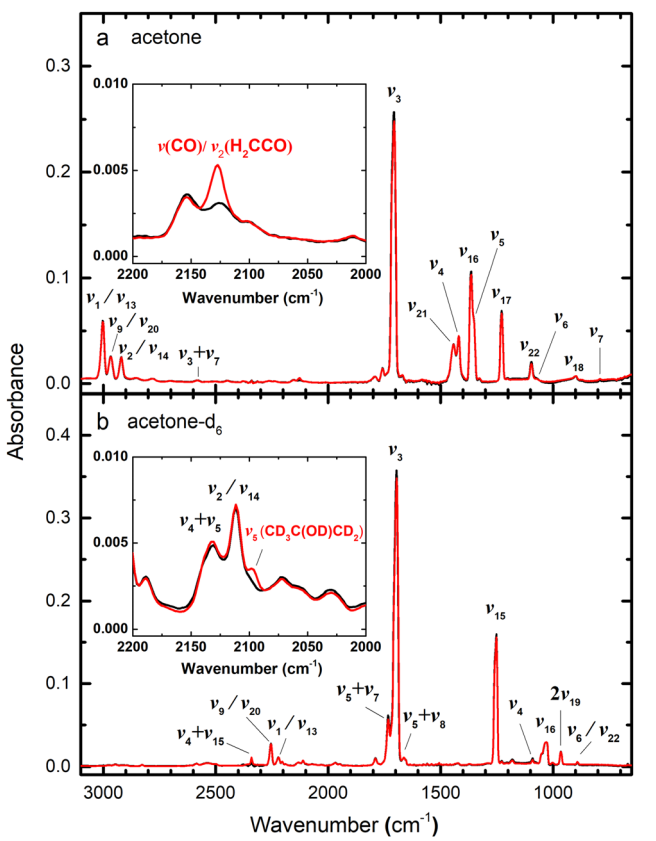

Fig. 2 FTIR spectra of acetone ices at 5 K before (black line) and after (red line) irradiation: (a) acetone, (b) acetone-d_6. Detailed assignments are compiled in Tables S4 and S5 (ESI†). Inset: Magnified view of 2200–2000 cm^{-1} showing new peaks after irradiation corresponding to carbon monoxide and/or ketene at 2128 cm^{-1} (a) and tentatively assigned propen-2-ol-d_6 at 2096 cm^{-1} (b).

with the formation of propen-2-ol (**2**). Since the infrared-active fundamentals of organics in complex mixtures often overlap with complex mixtures of organics formed in the processed ice, it is challenging to identify individual molecules using FTIR spectroscopy alone.[53–55] Therefore, an alternative technique, which has the ability to identify individual molecules isomer-selectively, is required.

PI-ReToF-MS

The firm detection of propen-2-ol (**2**) is accomplished through the photoionization reflectron time-of-flight mass spectrometry (PI-ReToF-MS) technique exploiting a tunable vacuum ultraviolet (VUV) light source.[54] Individual isomers were selectively ionized based on their ionization energies in the gas phase (Fig. 1) during the sublimation of the irradiated ices. The temperature-dependent mass spectra collected at distinct photon energies along with the blank experiment are compiled in Fig. 3; the corresponding TPD profiles are depicted in Fig. 4 and Fig. S1 (ESI†). Let us focus first on the ion signal at mass-to-charge ratio (m/z) of m/z = 58 ($C_3H_6O^+$) in the acetone system. At a photon energy of 9.43 eV (Fig. 4a), the TPD profile reveals a broad sublimation event centered at 148 K (peak 1) along with a shoulder extending to 210 K (peak 2). Note that the small peak at 166 K is assigned to the fragments from dissociative photoionization of m/z = 100, 116 and/or 158 species (Fig. S1, ESI†). Since the ion signal at m/z = 58 can be associated with the molecular formulae $C_2H_2O_2$, C_3H_6O, and C_4H_{10}, it is imperative to confirm the molecular formula through isotopically labeled reactants. In acetone-d_6 (CD_3COCD_3) ices, the TPD profile shifts by 6 amu from m/z = 58 to m/z = 64 (Fig. 4a); both TPD traces match very well indicating the presence of six hydrogen atoms and hence the molecular formula C_3H_6O.

The ion signal collected at 9.43 eV can be linked to multiple C_3H_6O isomers (Fig. 1): propen-2-ol (**2**, IE = 8.62–8.80 eV), methyl vinyl ether (**4**, IE = 8.91–8.93 eV), methoxy methyl carbene (**5**, CH_3OCCH_3; IE = 6.24–7.72 eV), and 1-methyleneoxyethyl (**6**, $H_2COCHCH_3$; IE = 6.45–7.27 eV). Acetone (**1**) and its isomer propylene oxide (**3**) cannot be ionized at 9.43 eV. A reduction of the photon energy to 8.90 eV, at which methyl vinyl ether (**4**) cannot be ionized, changes the TPD profile (Fig. 4c), and the late sublimation event (peak 2) is absent. Therefore, this high-temperature sublimation event can be linked to methyl vinyl ether (**4**), whereas peak 1 can be connected to propen-2-ol (**2**), methoxy methyl carbene (**5**) and/or 1-methyleneoxyethyl (**6**). Lowering the photon energy further to 8.40 eV eliminates peak 1

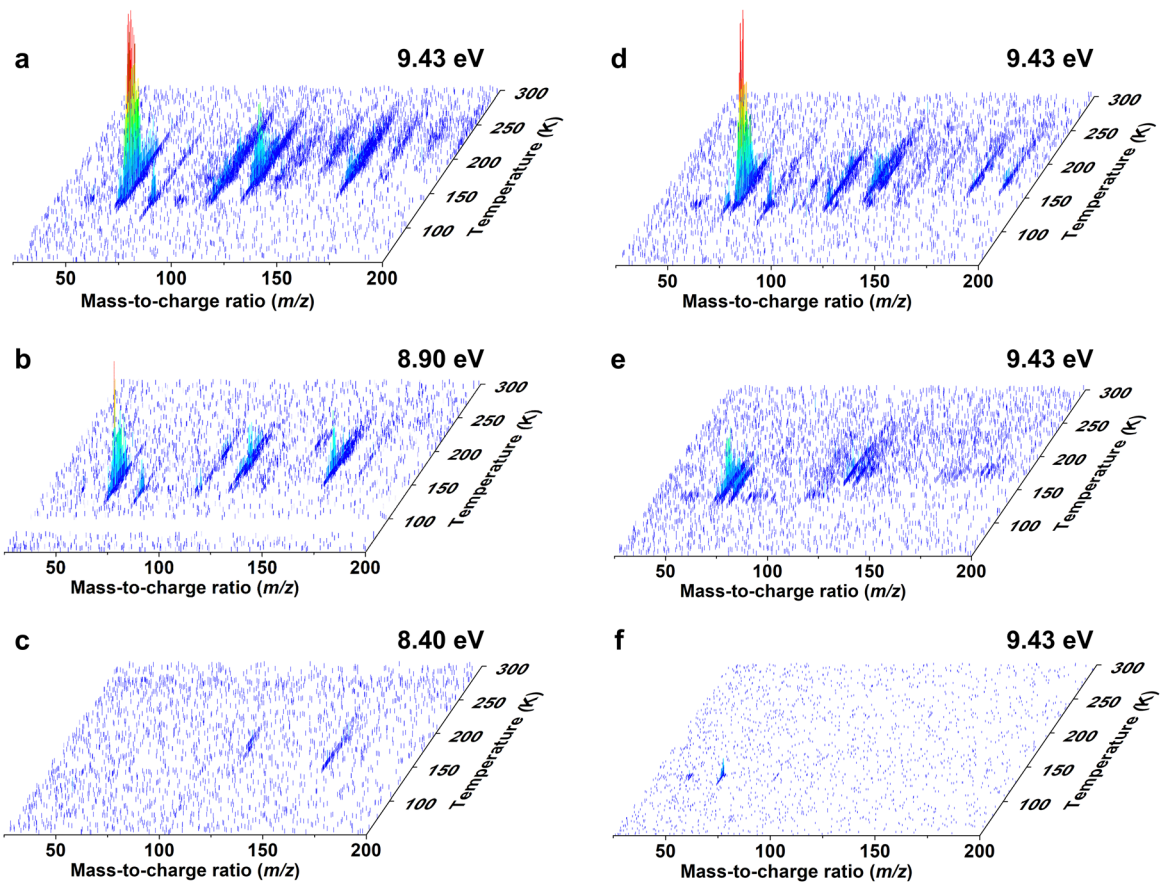

Fig. 3 PI-ReToF-MS mass spectra collected during the temperature-programmed desorption (TPD) of the irradiated ices. Data were recorded for the irradiated acetone ice at photon energies of 9.43 eV (a), 8.90 eV (b), and 8.40 eV (c), the irradiated acetone-d_6 ice at 9.43 eV (d) as well as the irradiated acetone–acetone-d_6 ice at 9.43 eV (e). The blank experiment of the acetone ice performed under identical conditions, but without irradiation, was recorded at 9.43 eV (f).

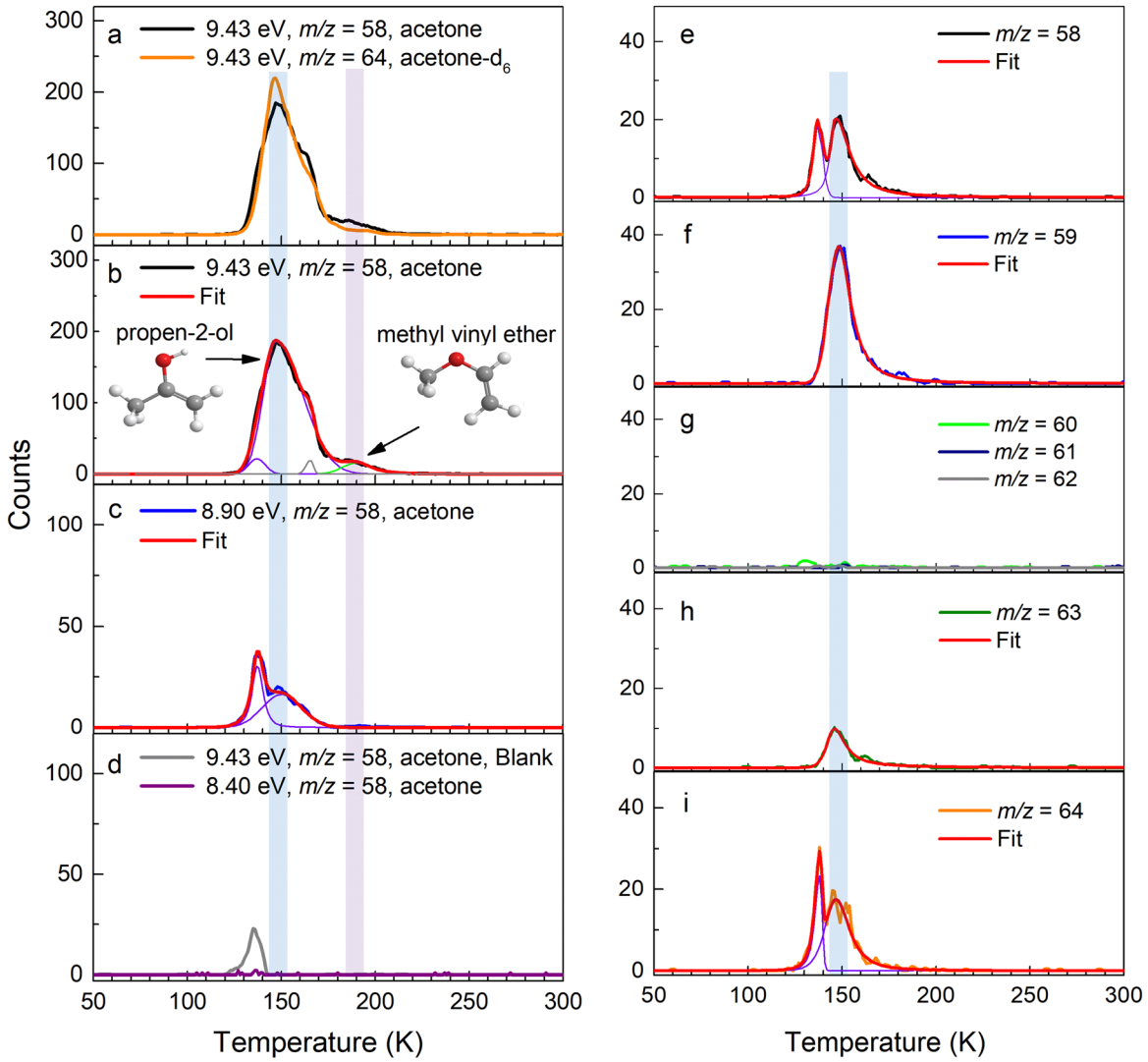

Fig. 4 PI-ReToF-MS data during the TPD phase measured for irradiated (0.34 ± 0.05 eV molecule^{-1}) acetone ice at m/z = 58 at photon energies of 9.43 eV (a and b), 8.90 eV (c) and 8.40 eV (d). Spectra of irradiated acetone-d_6 ice measured at m/z = 64 was recorded at 9.43 eV (a). The blank experiment acetone ice was recorded at 9.43 eV (d). Spectra of acetone–acetone-d_6 ice were recorded at 9.43 eV at m/z = 58 (e), m/z = 59 (f), m/z = 60–62 (g), m/z = 63 (h), and m/z = 64 (i) after lower dose irradiation (0.10 ± 0.02 eV molecule^{-1}). The blue and purple shaded regions indicate the peak positions corresponding to propen-2-ol (**2**) and methyl vinyl ether (**4**), respectively. The solid red lines indicate total fit of the spectra.

(Fig. 4d). Since the 8.40 eV photon can ionize **5** or **6**, but not propen-2-ol (**2**), the detection of methoxy methyl carbene (**5**) and 1-methyleneoxyethyl (**6**) can be ruled out, and the low temperature sublimation event can be assigned to propen-2-ol (**2**). Propen-2-ol (**2**) has two conformers in which the hydroxyl group is oriented either the same (*syn*-) or opposite (*anti*-) with respect to the double bond. The more stable conformer, *syn*-propen-2-ol, has a dipole moment of 0.54 D, which is smaller than that of methyl vinyl ether (0.98 D).[6] Therefore, propen-2-ol molecules could sublime at a lower temperature compared to methyl vinyl ether (**4**). It should be noted that in the blank experiment at 9.43 eV conducted under the same conditions, but without exposing the ices to ionizing radiation, a weak sublimation event that starts at 120 K, peaks at 136 K, and returns to the baseline level at 143 K (Fig. 4d). This signal is likely due to the natural abundance of propen-2-ol (**2**) in acetone samples.[56] In addition, Fig. S2 (ESI†) shows the peak sublimation temperature of acetone is at 137 K, indicating the weak sublimation event in the blank experiment is caused by the co-sublimation of acetone (**1**).

An additional experiment with acetone–acetone-d_6 ice was performed at a photon energy of 9.43 eV with a low dose of 0.10 ± 0.02 eV molecule^{-1} to gain mechanistic insights into the formation of propen-2-ol (**2**) by inspecting distinct levels of deuteration in the products (Fig. 4e–4i). Most notably, propen-2-ol-d_1 (C_3H_5DO, m/z = 59) forms at a higher abundance compared to propen-2-ol-d_5 (C_3HD_5O, m/z = 63) (Table S6, ESI†). Since no signal was detected at m/z = 60–62 (Fig. 4g), the exchange of more than one hydrogen/deuterium atoms does not proceed. In addition, ion signals at m/z = 72, 86, 100, 114, 116, and 158 in irradiated acetone ice were observed at 9.43 eV (Fig. S1 and S4, ESI†). The proposed formation pathways for the tentatively assigned molecules are shown in Fig. S5 and S6 (ESI†).

Electronic structure calculations

Having confirmed the synthesis of propen-2-ol (**2**) and methyl vinyl ether (**4**) *via* irradiation of acetone, we shift focus to elucidating the mechanisms of their formation. Propen-2-ol (**2**) can be formed *via* keto–enol tautomerization *via* intramolecular hydrogen transfers from the methyl group to the carbonyl oxygen atom in acetone (**1**). We explored computationally the potential energy surface at the higher CCSD(T)-F12/cc-pVTZ-F12//ωB97X-D/6-311G(d,p) level of theory. This study revealed that the overall enolization is endoergic by 50 kJ mol^{-1} (Fig. 5a); this data agrees well with a previous study (47 kJ mol^{-1}) determined at the CCSD(T,FULL)/aug-cc-pVTZ//CCSD(T)/6-31+G(d,p) level of theory.[57] In the gas-phase, this process has a high barrier to reaction of 274 kJ mol^{-1} indicating that excess energy from the impinging radiation is required to generate propen-2-ol (**2**).[7] Since nearby molecules in the ice phase could be involved in the reaction mechanism, gas-phase calculations may overestimate the real barrier of the reactions. For low-temperature reactions involving hydrogen and/or proton transfer processes, strong kinetic isotope effects are often associated with quantum mechanical tunneling (QMT).[58] However, under identical experimental conditions, the ion signals of propen-2-ol and propen-2-ol-d_6 were detected at similar levels (Table S6, ESI†). This finding suggests that isotopic substitution has no effect on the formation of propen-2-ol (**2**); therefore, QMT can be likely ruled out. Therefore, tautomerization leading to propen-2-ol (**2**) requires non-equilibrium reactions by imparting excess energy from the impinging electrons into the system so that the transition state to reaction can be efficiently passed.

In the gas-phase, methyl vinyl ether (**4**) has *syn*- and *anti*-conformers, with the *syn* conformer being 13 kJ mol^{-1} more stable.[6] The barrier from *syn*- to *anti*-methyl vinyl ether is calculated to be 28 kJ mol^{-1}. The formation of methyl vinyl ether (**4**) can proceed through two reaction pathways (Fig. 1a). The first pathway (red line) involves methoxy methyl carbene (**5**), which in turn can be accessed through migration of a methyl group to the oxygen atom of the carbonyl moiety over a barrier of 505 kJ mol^{-1}.[6] Methoxy methyl carbene (**5**) then isomerizes to *anti*-methyl vinyl ether (**4**) *via* a hydrogen shift from the methyl group to the carbene center. The second feasible pathway (blue line) involves isomerization of acetone (**1**) to propylene oxide (**3**) with a barrier of 444 kJ mol^{-1}. The ring of propylene oxide (**3**) then opens to yield 1-methyleneoxyethyl (**6**) followed by isomerization through an exotic 5-membered cyclic transition state to *syn*-methyl vinyl ether (**4**). Note that these barriers can be overcome by the energy contributed by energetic electrons. We conducted the photoionization of the subliming molecules from the irradiated acetone system at a photon energy of 10.49 eV; at this energy, propylene oxide (**3**) can be ionized. However, no propylene oxide (**3**) was detected. Therefore, the first pathway (red line) is preferred based on the experimental results.

The aforementioned computational studies were conducted in the gas phase. In the interstellar medium, water (H_2O) ice represents the main constituent of icy nanoparticles in cold molecular clouds.[59] Therefore it is educational to explore the role of water in the keto–enol tautomerization. Given that ketones and water are polar molecules, solvent effects may lower the reaction barrier of the formation of enol tautomers. To gain insight into the fundamental enolization process in the

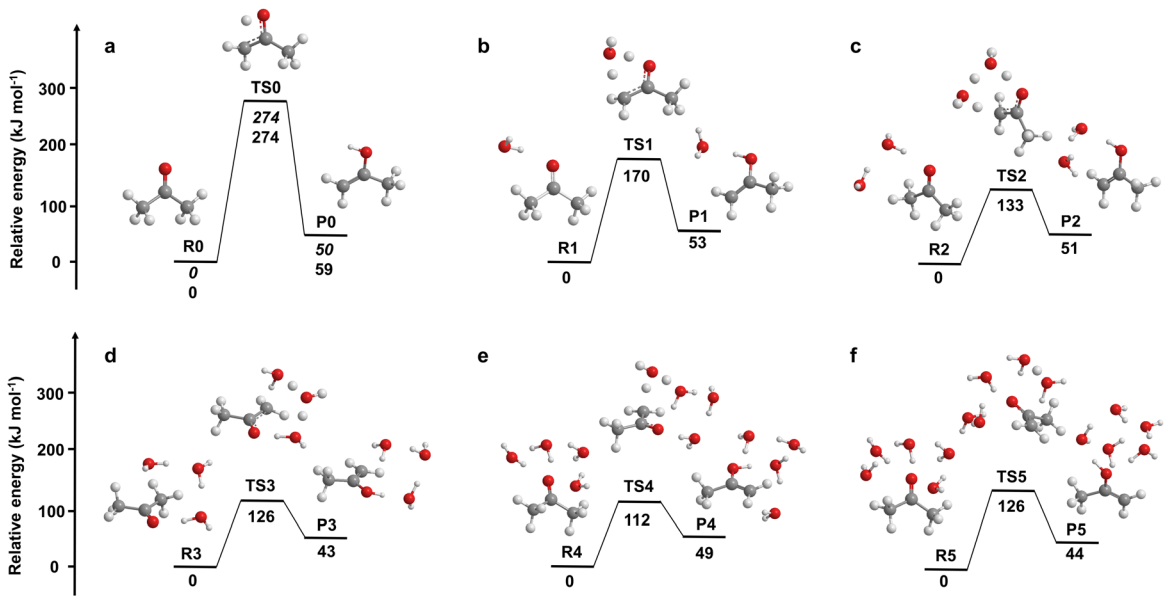

Fig. 5 Potential energy surfaces of reactions between acetone and water molecules leading to the formation of propen-2-ol (**2**). Panel (a) describes the gas-phase keto–enol tautomerization reaction of acetone (**1**). Panels (b)–(f) show the tautomerization reaction in the presence of 1–5 microsolvating water molecules with the inclusion of polarizable continuum model (PCM) solvent modeling to best replicate the condensed-phase environment of interstellar ices. In the case of five molecules participating (f), only three of them are directly involved in the H transfer transition state and two serve as microsolvents. A transition state with all five H_2O molecules involved in the H transfer also exists but corresponds to a higher barrier of 138 kJ mol^{-1}. Energies (kJ mol^{-1}) are calculated at the ωB97X-D/6-311G(d,p) level with CCSD(T)-F12/cc-pVTZ-F12 single-point corrected energies are in italics.

condensed phase, we performed electronic structure calculations for the reactions of acetone (CH_3COCH_3) and water molecules at the ωB97X-D/6-311G(d,p) level of theory with the use of self-consistent reaction field (SCRF) and polarizable continuum model (PCM) (Fig. 5b–5f). PCM utilizes a series of overlapping spheres to create the solute cavity and represents one of the most successful approaches to be combined with a quantum–mechanical description of the molecular solute.[60] All transition states were confirmed by intrinsic reaction coordinate (IRC) calculations. The tautomerization barriers for the $CH_3COCH_3/n(H_2O)$ (n = 0–5) systems decrease substantially from 274 kJ mol^{-1} to 112 kJ mol^{-1} (Fig. S3, ESI†) thus highlighting the solvent effects of water molecules. It is worth noting that the formation barriers of 1,3-dioxolane-4-ol ($C_3H_6O_3$) resulting from the addition of glycolaldehyde ($HCOCH_2OH$) to formaldehyde (H_2CO) are lowered by almost 84 kJ mol^{-1} with a water molecule involved in the reaction, which is predominantly governed by tunneling at lower temperatures.[61] The barrier height in the CH_3COCH_3–$(H_2O)_n$ systems essentially levels off for n = 2 indicating that barrier reduction in the reactions is caused by the direct involvement of water molecules rather than the interaction with the dipole field of the polar solvent. In fact, with one or more water molecules present, the hydrogen atom transfer process in the keto–enol isomerization (from the methyl group to the carbonyl oxygen atom) involves water species. With one water present, a hydrogen atom transfers from the methyl moiety to water, whereas another hydrogen atom shifts from water to the carbonyl group. With more than one water molecules participating, they form a chain between the CH_3 and C═O groups, and the hydrogen atom transfers occur simultaneously in this chain, from CH_3 to the first water in the chain, between water molecules along the chain, and finally, from the last water to the carbonyl moiety. This results in the barrier decrease by more than a factor of two. In the meantime, a comparison of the barrier heights computed without and with SCRF-PCM show that the implicit solvent effects, *i.e.*, the influences of the solvent dipole field on the barrier height, are minimal and do not exceed 10 kJ mol^{-1} being thus within the accuracy of the theoretical methods used. Future experiments incorporating water into the acetone ice will be needed to better understand the keto–enol tautomerization processes in interstellar ices.

Conclusions

Our combined experimental and computational study reveals the first preparation of the hitherto astronomically elusive propen-2-ol (**2**) and methyl vinyl ether (**4**) isomers in low-temperature acetone (**1**) ices upon exposure to proxies of galactic cosmic rays. Both isomers were detected in the gas-phase upon sublimation of the exposed ices exploiting tunable VUV photoionization coupled with reflectron time-of-flight mass spectrometry. Our electronic structure calculations provide compelling evidence that on 'real' interstellar grains, the barrier of the keto–enol tautomerization can be reduced by more than a factor of two through the involvement of water molecules thus highlighting the critical role of solvent effects in low-temperature ices. Once formed in interstellar ices, such molecules can sublime into the gas phase in the star-forming region, where they can be searched for by telescopes such as the James Webb Space Telescope. The first identification of propen-2-ol (**2**) from acetone (**1**) under simulated conditions replicating the interaction of ionizing radiation with ices on interstellar grains has far reaching implications to better understand the complex organic chemistry in deep space. Due to their nucleophilic character and high reactivity,[14] enols are anticipated playing a crucial role in the synthesis of complex organics such as sugars thus advancing the chemical complexity of the interstellar medium.[62] These prebiotic molecules can be eventually incorporated into comets and meteorites and be delivered to planets such as the early Earth[63] thus contributing to the synthesis of precursors linked to the Origin of Life.

Author contributions

R. I. K. designed the experiments and directed the project. J. W., C. Z., and J. H. M. performed experiments. J. W. performed the data analyses. A. A. N, V. N. A., A. K. E., and A. M. M. carried out the theoretical calculations. J. W., A. M. M., and R. I. K. wrote the manuscript, which was read, revised, and approved by all co-authors.

Data availability

Essential data are provided in the main text and the ESI.† Additional data can be available from the corresponding author upon reasonable request.

Conflicts of interest

The authors declare no conflict of interest.

Acknowledgements

Experiments were supported by US National Science Foundation, Division of Astronomical Sciences under grant AST-2103269 awarded to the University of Hawaii at Manoa (R. I. K.). The experimental setup was financed by W. M. Keck Foundation and the University of Hawaii at Manoa. A. K. E. thanks the Fonds der Chemischen Industrie (Liebig Fellowship) and the Deutsche Forschungsgemeinschaft (DFG, German Research Foundation) under Germany's Excellence Strategy – EXC-2033 – 390677874 - RESOLV for funding. The calculations of the reaction potential energy surfaces were supported by the Ministry of Higher Education and Science of the Russian Federation under grant No. 075-15-2021-597.

References

1 E. Erlenmeyer, *Ber. Dtsch. Chem. Ges.*, 1880, **13**, 305–310.
2 G. R. McMillan, J. G. Calvert and J. N. Pitts, *J. Am. Chem. Soc.*, 1964, **86**, 3602–3605.

3 C. A. Taatjes, N. Hansen, A. McIlroy, J. A. Miller, J. P. Senosiain, S. J. Klippenstein, F. Qi, L. Sheng, Y. Zhang, T. A. Cool, J. Wang, P. R. Westmoreland, M. E. Law, T. Kasper and K. Kohse-Höinghaus, *Science*, 2005, **308**, 1887–1889.
4 D. U. Andrews, B. R. Heazlewood, A. T. Maccarone, T. Conroy, R. J. Payne, M. J. T. Jordan and S. H. Kable, *Science*, 2012, **337**, 1203–1206.
5 C.-W. Zhou, Z.-R. Li and X.-Y. Li, *J. Phys. Chem. A*, 2009, **113**, 2372–2382.
6 M. Elango, G. S. Maciel, F. Palazzetti, A. Lombardi and V. Aquilanti, *J. Phys. Chem. A*, 2010, **114**, 9864–9874.
7 M. J. Abplanalp, S. Gozem, A. I. Krylov, C. N. Shingledecker, E. Herbst and R. I. Kaiser, *Proc. Natl. Acad. Sci. U. S. A.*, 2016, **113**, 7727–7732.
8 N. F. Kleimeier, A. K. Eckhardt, P. R. Schreiner and R. I. Kaiser, *Chem*, 2020, **6**, 3385–3395.
9 N. F. Kleimeier, A. K. Eckhardt and R. I. Kaiser, *J. Am. Chem. Soc.*, 2021, **143**, 14009–14018.
10 N. F. Kleimeier and R. I. Kaiser, *J. Phys. Chem. Lett.*, 2022, **13**, 229–235.
11 R. Breslow, *Tetrahedron Lett.*, 1959, **1**, 22–26.
12 G. da Silva, *Angew. Chem., Int. Ed.*, 2010, **49**, 7523–7525.
13 K. O. Johansson, T. Dillstrom, M. Monti, F. El Gabaly, M. F. Campbell, P. E. Schrader, D. M. Popolan-Vaida, N. K. Richards-Henderson, K. R. Wilson, A. Violi and H. A. Michelsen, *Proc. Natl. Acad. Sci. U. S. A.*, 2016, **113**, 8374–8379.
14 H. Hart, *Chem. Rev.*, 1979, **79**, 515–528.
15 B. E. Turner and A. J. Apponi, *Astrophys. J.*, 2001, **561**, L207–L210.
16 A. M. Turner, A. S. Koutsogiannis, N. F. Kleimeier, A. Bergantini, C. Zhu, R. C. Fortenberry and R. I. Kaiser, *Astrophys. J.*, 2020, **896**, 88.
17 J. Wang, J. H. Marks, A. M. Turner, A. A. Nikolayev, V. Azyazov, A. M. Mebel and R. I. Kaiser, *Phys. Chem. Chem. Phys.*, 2023, **25**, 936–953.
18 V. M. Rivilla, L. Colzi, I. Jiménez-Serra, J. Martín-Pintado, A. Megías, M. Melosso, L. Bizzocchi, Á. López-Gallifa, A. Martínez-Henares, S. Massalkhi, B. Tercero, P. de Vicente, J.-C. Guillemin, J. García de la Concepción, F. Rico-Villas, S. Zeng, S. Martín, M. A. Requena-Torres, F. Tonolo, S. Alessandrini, L. Dore, V. Barone and C. Puzzarini, *Astrophys. J., Lett.*, 2022, **929**, L11.
19 G. P. Laroff and H. Fischer, *Helv. Chim. Acta*, 1973, **56**, 2011–2020.
20 J. L. Holmes and F. P. Lossing, *J. Am. Chem. Soc.*, 1982, **104**, 2648–2649.
21 X. K. Zhang, J. M. Parnis, E. G. Lewars and R. E. March, *Can. J. Chem.*, 1997, **75**, 276–284.
22 M. F. Shaw, D. L. Osborn, M. J. T. Jordan and S. H. Kable, *J. Phys. Chem. A*, 2017, **121**, 3679–3688.
23 K. Hiraoka, A. Yamashita, T. Miyagoshi, N. Oohashi, Y. Kihara and K. Yamamoto, *Astrophys. J.*, 1998, **508**, 423.
24 D. P. P. Andrade, A. L. F. de Barros, J. Ding, H. Rothard, P. Boduch and E. F. da Silveira, *Mon. Not. R. Astron. Soc.*, 2014, **444**, 3792–3801.
25 R. L. Hudson, *Phys. Chem. Chem. Phys.*, 2018, **20**, 5389–5398.
26 G. A. Carvalho and S. Pilling, *Mon. Not. R. Astron. Soc.*, 2020, **498**, 689–701.
27 X. S. Xu, Z. Hu, M. X. Jin, H. Liu and D. Ding, *J. Mol. Struct.*, 2003, **638**, 215–228.
28 A. G. Yeghikyan, *Astrophysics*, 2011, **54**, 87–99.
29 F. Combes, M. Gerin, A. Wootten, G. Wlodarczak, F. Clausset and P. J. Encrenaz, *Astron. Astrophys.*, 1987, **180**, L13–L16.
30 L. E. Snyder, F. J. Lovas, D. M. Mehringer, N. Y. Miao, Y.-J. Kuan, J. M. Hollis and P. R. Jewell, *Astrophys. J.*, 2002, **578**, 245.
31 M. K. McClure, W. R. M. Rocha, K. M. Pontoppidan, N. Crouzet, L. E. U. Chu, E. Dartois, T. Lamberts, J. A. Noble, Y. J. Pendleton, G. Perotti, D. Qasim, M. G. Rachid, Z. L. Smith, F. Sun, T. L. Beck, A. C. A. Boogert, W. A. Brown, P. Caselli, S. B. Charnley, H. M. Cuppen, H. Dickinson, M. N. Drozdovskaya, E. Egami, J. Erkal, H. Fraser, R. T. Garrod, D. Harsono, S. Ioppolo, I. Jiménez-Serra, M. Jin, J. K. Jørgensen, L. E. Kristensen, D. C. Lis, M. R. S. McCoustra, B. A. McGuire, G. J. Melnick, K. I. Öberg, M. E. Palumbo, T. Shimonishi, J. A. Sturm, E. F. van Dishoeck and H. Linnartz, *Nat. Astron.*, 2023, **7**, 431–443.
32 B. M. Jones and R. I. Kaiser, *J. Phys. Chem. Lett.*, 2013, **4**, 1965–1971.
33 A. M. Turner, M. J. Abplanalp, S. Y. Chen, Y. T. Chen, A. H. Chang and R. I. Kaiser, *Phys. Chem. Chem. Phys.*, 2015, **17**, 27281–27291.
34 R. L. Hudson, P. A. Gerakines and R. F. Ferrante, *Spectrochim. Acta, Part A*, 2018, **193**, 33–39.
35 D. Drouin, A. R. Couture, D. Joly, X. Tastet, V. Aimez and R. Gauvin, *Scanning*, 2007, **29**, 92–101.
36 M. J. Frisch, G. W. Trucks, H. B. Schlegel, G. E. Scuseria, M. A. Robb, J. R. Cheeseman, G. Scalmani, V. Barone, G. A. Petersson, H. Nakatsuji, X. Li, M. Caricato, A. V. Marenich, J. Bloino, B. G. Janesko, R. Gomperts, B. Mennucci, H. P. Hratchian, J. V. Ortiz, A. F. Izmaylov, J. L. Sonnenberg, D. Williams-Young, F. Ding, F. Lipparini, F. Egidi, J. Goings, B. Peng, A. Petrone, T. Henderson, D. Ranasinghe, V. G. Zakrzewski, J. Gao, N. Rega, G. Zheng, W. Liang, M. Hada, M. Ehara, K. Toyota, R. Fukuda, J. Hasegawa, M. Ishida, T. Nakajima, Y. Honda, O. Kitao, H. Nakai, T. Vreven, K. Throssell, J. A. Montgomery Jr., J. E. Peralta, F. Ogliaro, M. J. Bearpark, J. J. Heyd, E. N. Brothers, K. N. Kudin, V. N. Staroverov, T. A. Keith, R. Kobayashi, J. Normand, K. Raghavachari, A. P. Rendell, J. C. Burant, S. S. Iyengar, J. Tomasi, M. Cossi, J. M. Millam, M. Klene, C. Adamo, R. Cammi, J. W. Ochterski, R. L. Martin, K. Morokuma, O. Farkas, J. B. Foresman and D. J. Fox, *GAUSSIAN 09, Revision A.1*, Gaussian Inc., Wallingford CT, 2009.
37 A. D. Becke, *Phys. Rev. A: At., Mol., Opt. Phys.*, 1988, **38**, 3098–3100.
38 A. D. Becke, *J. Chem. Phys.*, 1993, **98**, 5648–5652.
39 C. Lee, W. Yang and R. G. Parr, *Phys. Rev. B: Condens. Matter Mater. Phys.*, 1988, **37**, 785–789.
40 T. H. Dunning, *J. Chem. Phys.*, 1989, **90**, 1007–1023.

41 J. Čížek, *J. Chem. Phys.*, 1966, **45**, 4256–4266.
42 R. J. Bartlett, J. D. Watts, S. A. Kucharski and J. Noga, *Chem. Phys. Lett.*, 1990, **165**, 513–522.
43 K. Raghavachari, *Annu. Rev. Phys. Chem.*, 1991, **42**, 615–642.
44 J. F. Stanton, *Chem. Phys. Lett.*, 1997, **281**, 130–134.
45 K. A. Peterson, D. E. Woon and T. H. Dunning. Jr., *J. Chem. Phys.*, 1994, **100**, 7410–7415.
46 J.-D. Chai and M. Head-Gordon, *Phys. Chem. Chem. Phys.*, 2008, **10**, 6615–6620.
47 G. Knizia, T. B. Adler and H.-J. Werner, *J. Chem. Phys.*, 2009, **130**, 054104.
48 T. B. Adler, G. Knizia and H.-J. Werner, *J. Chem. Phys.*, 2007, **127**, 221106.
49 J. Tomasi, B. Mennucci and R. Cammi, *Chem. Rev.*, 2005, **105**, 2999–3094.
50 H.-J. Werner, P. J. Knowles, R. Lindh, F. R. Manby, M. Schütz, P. Celani, T. Korona, G. Rauhut, R. D. Amos and A. Bernhardsson, University of Cardiff: Cardiff, UK, 2010.
51 W. C. Harris and I. W. Levin, *J. Mol. Spectrosc.*, 1972, **43**, 117–127.
52 O. Berg and G. E. Ewing, *J. Phys. Chem.*, 1991, **95**, 2908–2916.
53 J. Wang, J. H. Marks, L. B. Tuli, A. M. Mebel, V. N. Azyazov and R. I. Kaiser, *J. Phys. Chem. A*, 2022, **126**, 9699–9708.
54 A. M. Turner and R. I. Kaiser, *Acc. Chem. Res.*, 2020, **53**, 2791–2805.
55 M. J. Abplanalp, M. Forstel and R. I. Kaiser, *Chem. Phys. Lett.*, 2016, **644**, 79–98.
56 S. I. Vlasov and A. V. Ponomarev, *Radiat. Phys. Chem.*, 2021, **184**, 109460.
57 E. Grajales-González, M. Monge-Palacios and S. M. Sarathy, *J. Phys. Chem. A*, 2018, **122**, 3547–3555.
58 H. Hidaka, A. Kouchi and N. Watanabe, *J. Chem. Phys.*, 2007, **126**, 204707.
59 D. C. B. Whittet, P. A. Gerakines, A. G. G. M. Tielens, A. J. Adamson, A. C. A. Boogert, J. E. Chiar, T. de Graauw, P. Ehrenfreund, T. Prusti, W. A. Schutte, B. Vandenbussche and E. F. van Dishoeck, *Astrophys. J.*, 1998, **498**, L159.
60 B. Mennucci, *Wiley Interdiscip. Rev.: Comput. Mol. Sci.*, 2012, **2**, 386–404.
61 A. K. Eckhardt, R. C. Wende and P. R. Schreiner, *J. Am. Chem. Soc.*, 2018, **140**, 12333–12336.
62 N. F. Kleimeier and R. I. Kaiser, *ChemPhysChem*, 2021, **22**, 1229–1236.
63 G. Cooper, N. Kimmich, W. Belisle, J. Sarinana, K. Brabham and L. Garrel, *Nature*, 2001, **414**, 879–883.